

A Strategy for the Mapping of *N*-Glycans by High-Performance Capillary Electrophoresis¹

Peter Hermentin,* Reiner Doenges,* Reinhild Witzel,* Cornelis H. Hokke,† Johannes F. G. Vliegthart,† Johannes P. Kamerling,† Harald S. Conradt,‡ Manfred Nimtz,‡ and Dieter Brazel*

*Research Laboratories of Behringwerke AG, P.O. Box 1140, D-35001 Marburg, Federal Republic of Germany; †Utrecht University, Bijvoet Center, Department of Bio-Organic Chemistry, P.O. Box 80075, NL-3508TB Utrecht, The Netherlands; and ‡Gesellschaft für Biotechnologische Forschung mbH, Department of Genetics, Mascheroder Weg 1, D-38124 Braunschweig, Federal Republic of Germany

Received December 20, 1993

We have evaluated high-performance capillary electrophoresis (HPCE) with respect to its suitability for use in establishing a carbohydrate-mapping database that would enable a carbohydrate structural analysis by mere comparison of migration times. The suitability of HPCE for carbohydrate structural assignments was ascertained by validation experiments. The migration times of distinct *N*-glycans, prepared and measured on different days, were shown to be highly reproducible, with a coefficient of variation of usually less than 0.20%, requiring only femtomoles of *N*-glycan per injection for reliable measurements. By including mesityl oxide and sialic acid as internal standards and a triple-correction method, HPCE fulfills the analytical requirements with respect to accuracy, precision, reproducibility, and sensitivity. The *N*-glycan-mapping database was established using a newly developed and optimized buffer system containing 1,5-diaminopentane as an organic modifier. Approximately 80 different sialylated *N*-glycans of known structure, which have thus far been measured and characterized, have been entered into our Lotus 1-2-3 mapping database. The database for structural determinations was tested using the *N*-linked carbohydrates released from recombinant human urinary erythropoietin (baby hamster kidney) by PNGase F treatment and from bovine serum fetuin and α_1 -acid glycoprotein by automated and manual (large-scale) hydrazinolysis, respectively. The efficiency of the database and of the triple-correction method was further confirmed by HPCE measurements performed in a different laboratory and by a different analyst who

used the HPCE system of a different manufacturer.

© 1994 Academic Press, Inc.

The demand for reproducible, fast, and facile carbohydrate analysis is increasing steadily. However, the structural analysis of complex carbohydrates requires expertise and the infrastructure for methylation analysis/GC-MS², FAB-MS, and high-resolution ¹H NMR spectroscopy. Therefore, an alternative that should allow the reduction of these high-cost and time-consuming demands of carbohydrate structural analysis by using standard separation techniques and affordable hardware appears attractive. We have previously shown that high-pH anion-exchange chromatography with pulsed amperometric detection (HPAE-PAD) fulfills the criteria for such a purpose (1).

In the search for an alternative mapping dimension,

² Abbreviations used: GC-MS, gas chromatography in combination with mass spectrometry; FAB-MS, fast atom bombardment-mass spectrometry; HPCE, high-performance capillary electrophoresis; HPAE-PAD, high-pH anion-exchange chromatography with pulsed amperometric detection; RT, migration time (i.e., retention time); SD, standard deviation; CV, coefficient of variation; TCM, triple-correction method; 2-AP, 2-aminopyridine; PA, pyridylaminated; 6-AQ, 6-aminoquinoline; AGA, amido-G-acid (7-amino-1,3-naphthalene disulfonic acid); CBQCA, 3-(4-carboxybenzoyl)-2-quinolinecarboxaldehyde; AGP, α_1 -acid glycoprotein; MQ, Mono-Q; d.p., degree of polymerization; MO, mesityl oxide; Neu5Ac, *N*-acetylneuraminic acid; S, sialic acid; G and Gal, D-galactose; N and GlcNAc, *N*-acetyl-D-glucosamine; M and Man, D-mannose; F and Fuc, L-fucose; LacNAc, *N*-acetylglucosamine; rhuEPO, recombinant human urinary erythropoietin; BHK, baby hamster kidney; rt-PA, recombinant tissue plasminogen activator; PTFE, polytetrafluoroethylene; FPLC, fast protein liquid chromatography; PNGase F, polypeptide: *N*-glycosidase F.

¹ A preliminary report was presented at the 2nd International Glycobiology Symposium: Current Analytical Methods, February 13-16, 1994, San Francisco, CA.

we have recently introduced HPCE with uv detection at 190 nm for the mapping of sialylated *N*-glycans, which consumed about 4000 times less material than the mapping by HPAE-PAD (2). The newly developed HPCE buffer system (i.e., 80 mM ammonium sulfate, 20 mM sodium phosphate, 2 mM 1,4-diaminobutane, adjusted to pH 7.0 with phosphoric acid (2)) was further improved by replacing the organic modifier, 1,4-diaminobutane, with 1,5-diaminopentane and by adjusting the buffer to pH 7.0 with 1 N sulfuric acid (instead of phosphoric acid).

Here we describe a method that makes it possible to measure the migration times of *N*-glycans with coefficients of variation of usually less than 0.20%. The high accuracy achieved enabled us to initiate and build a validated HPCE-mapping database that allows structural assignments of sialylated *N*-glycans by mere comparison of their corrected HPCE migration (or retention) times. This extraordinary validity of the HPCE migration times (CV < 0.20%) was achieved using two internal standards and a triple-correction of the measured RTs of the samples. The technique was validated using the hydrazinolysis-derived *N*-glycan pool of human plasma α_1 -acid glycoprotein (AGP).

The HPCE-mapping database was initiated with approximately 80 different *N*-glycans that were isolated from purified glycoproteins or tryptic digests thereof according to known procedures, and the structures were determined by methylation analysis, FAB-MS, and ^1H NMR spectroscopy (3–12). Additional *N*-glycans were purchased as available. The efficiency of the database was examined by the structural assignment of the sialylated *N*-glycans of rhuEPO (BHK), isolated via PNGase F treatment, as well as of bovine serum fetuin and AGP, liberated via automated and manual (large-scale) hydrazinolysis, respectively.

EXPERIMENTAL

Chemicals

The following chemicals were purchased from Merck: ammonium sulfate, ammonium acetate, calcium chloride, disodium hydrogen phosphate, phosphoric acid, and mesityl oxide. 1,4-Diaminobutane and 1,5-diaminopentane were purchased from Fluka. Sodium hydroxide was from Riedel-de-Haen, Neu5Ac from Sigma, PNGase F from Boehringer-Mannheim, AGP (Lot 281184) from Behringwerke AG, and bovine serum fetuin from Oxford GlycoSystems (Abingdon, England). The rhuEPO (BHK) was from Merckle GmbH (Ulm, FRG) and represents a pharmaceutically developed product of Elanex Pharmaceuticals (Bothell, U.S.A.).

Preparation of the Glycan Pools

Two hydrazinolysis-derived AGP *N*-glycan pools were prepared from 50 and 1000 mg of AGP by conventional hydrazinolysis, as described elsewhere (2).

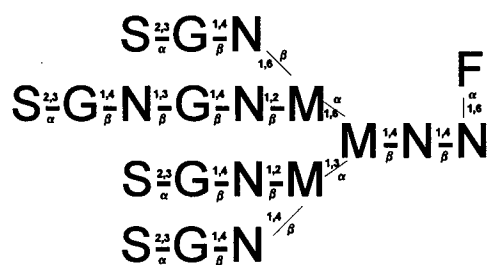
The hydrazinolysis-derived fetuin glycan pool was prepared from 2 mg of fetuin using an automated glycan release and recovery apparatus (GlycoPrep 1000, Oxford GlycoSystems), the standard chemicals and equipment provided, and the "N + O" mode (for the total glycan release). The recovered *N*-glycan solution (4.6 ml) was buffered by the addition of aq sodium acetate (0.5 ml), filtered through a 0.22- μm PTFE filter, and concentrated to dryness in a SpeedVac overnight. The remainder was desalted via Sephadex G-25 (Pharmacia, Uppsala, Sweden), again concentrated to dryness in a SpeedVac, taken up in distilled water (200 μl), and kept frozen at -20°C until further use. The fetuin *O*-glycans liberated during hydrazinolysis were largely removed during the desalting step.

The liberation by PNGase F of the EPO *N*-glycans was as described by Nimtz and colleagues (7).

HPCE Apparatus and Conditions

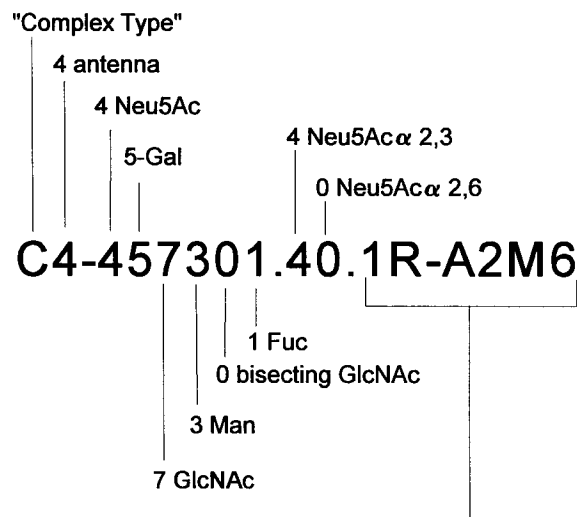
The HPCE measurements were performed, if not stated otherwise, with an Applied Biosystems 270A-HT capillary electrophoresis apparatus, working with a fused-silica capillary of 50 μm i.d. and 365 μm o.d. and an effective length of 100 cm (Supelco, Bellefonte, PA); buffer system: 80 mM ammonium sulfate, 20 mM sodium phosphate, 2.0 mM 1,5-diaminopentane, adjusted with 1 N sulfuric acid to pH 7.0. The normal polarity technique was used, in which the sample is applied at the anodic side. If not stated otherwise, the runs were performed at 30°C at 20 kV, corresponding to a current of 70 μA , and oligosaccharides were detected at 190 nm. The electropherograms were recorded via a Perkin-Elmer 900 series interface using the Nelson PC-integrator software version 5.1. Prior to use, the new capillary was equilibrated with 1 M sodium hydroxide for 2 h, with water for 15 min, and finally with running buffer for 30 min. Between individual runs, the capillary was rinsed with running buffer for 5 min using a 20-in. vacuum at the cathodic side. If not stated otherwise, mesityl oxide (1:200, v/v in water) and Neu5Ac (500 $\mu\text{g}/\text{ml}$ in water) were used as internal standards. The samples were loaded for 1, 2, or 5 s by vacuum injection, using a 5-in. vacuum (16.9 kPa), corresponding to a sample volume of 1, 2, or 5 nl, respectively. The standards were similarly loaded from different vessels in the amounts of 1 or 2 nl.

Alternatively, HPCE measurements of the AGP *N*-glycan pool were also performed with a Beckman 5500 P/ACE system equipped with the Beckmann System Gold software. The capillary cassette was fitted with a



C2-124301.01.60.

SCHEME 3. Proposed nomenclature of diantennary N-glycans.

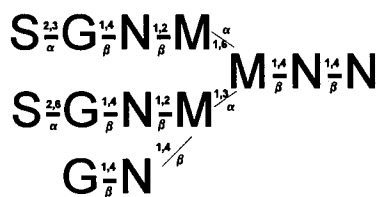


SCHEME 1. Proposed nomenclature of tetraantennary N-glycans (adapted from Ref. 1).

50- μ m i.d. fused-silica capillary (Supelco) 107 cm in length (100 cm to the detector). Injections of the sample and the standards were achieved using low pressure (0.5 psi) for 5 and 1 s, respectively. The temperature was controlled at $30 \pm 0.1^\circ\text{C}$. The runs were performed at 30 kV; detection was at 194 ± 4 nm.

Database Nomenclature of N-Glycans

The nomenclature of the N-glycans was as previously described (1) and is schematically outlined in Scheme 1



C3-235300.11.A4M3.360.

SCHEME 2. Proposed nomenclature of triantennary N-glycans.

(for a distinct tetraantennary structure), Scheme 2 (for a distinct triantennary isomer), and Scheme 3 (for a distinct diantennary N-glycan), respectively.

Nomenclature terms abbreviated with an asterisk indicate groups of structures defined by the initials preceding the star; e.g., the abbreviations C4*, C3*, and C2* reflect all tetra-, tri-, and diantennary complex type N-glycan structures, respectively, irrespective of their degree of sialylation. On the other hand, C4-4*, C4-3*, and C4-2* refer to tetraantennary N-glycans carrying four, three, and two sialic acid residues, respectively. The abbreviations C3-3* and C3-2* denote triantennary complex type N-glycans with three and two Neu5Ac residues, respectively. The terms C2-2* and C2-1* correspond to diantennary disialo and monosialo complex type N-glycans, respectively.

Question marks indicate ambiguities; e.g., C3-235300.??A4M3 codes for the group of disialo-triantennary nonfucosylated sialyl isomers of the A4M3-type branching in which the antenna is attached to position 4 of the mannose which is α 1,3-linked. A distinct example of this group is C3-235300.11.A4M3.360. (Scheme 2), in which "11.A4M3" reflects the presence of one α 2,3- and one α 2,6-linked Neu5Ac residue. The suffix "A4M3-360." relates to the distinct sialic acid linkage and branch location: The first digit, 3, refers to an α 2,3-linked Neu5Ac at the "upper" ("A2M6") branch. The second digit, 6, reflects an α 2,6-linkage of Neu5Ac at the "middle" ("A2M3") branch. The third digit, 0, indicates that the "lower" ("A4M3") branch is lacking Neu5Ac.

Similarly, C2-124301.01.60. refers to the monosialylated diantennary fucosylated complex type N-glycan with one α 2,6-linked Neu5Ac, which is located at the "upper" ("A2M6") branch (Scheme 3).

Oligosaccharides

N-Glycans were liberated from distinct glycoproteins by PNGase F treatment and isolated by FPLC/Mono-Q (Pharmacia, Uppsala, Sweden), followed by HPLC on an NH₂-bonded phase (Lichrosorb-NH₂, Merck, Darmstadt, FRG) (6,10). The detailed structural analysis of these N-linked oligosaccharides was performed by GC-MS (methylation and compositional analysis), FAB-

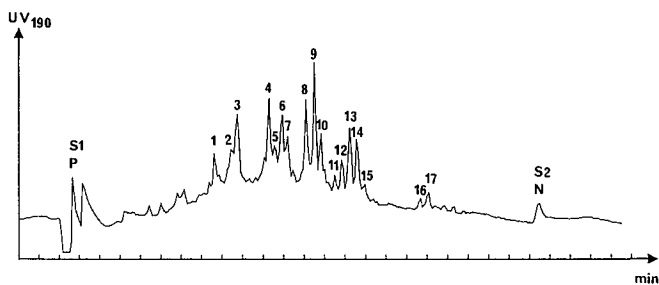


FIG. 1. Electropherogram of the large-scale hydrazinolysis-derived *N*-glycan pool of human plasma AGP (50 mg scale). S1, internal standard 1 (buffer peak); S2, internal standard 2 (Neu5Ac).

MS, and ^1H NMR spectroscopy (3–12). Other *N*-glycans were purchased from Oxford GlycoSystems or from Dionex (Sunnyvale, CA), as available.

Database Standards

The database was built with reference to mesityl oxide and Neu5Ac as internal standards and their “fix” migration times of 29.891 ± 0.374 min (CV 1.25%) and 52.959 ± 1.127 min (CV 2.13%), respectively, as determined from 65 consecutive runs (not shown).

Triple-Correction Method

The algorithm of the TCM comprises the following three equations:

Correction 1

$$C1 = RT_m / S1_m \times S1_{fx} \quad [1]$$

Correction 2

$$C2 = RT_m / S2_m \times S2_{fx} \quad [2]$$

Correction 3

$$C3 = (C1 + C2) / 2, \quad [3]$$

where RT_m is RT measured for the material; $C1$, RT_m , corrected via standard 1; $S1_m$, RT measured for internal standard 1; $S1_{fx}$, fixed standard RT of standard 1; $C2$, RT_m , corrected via standard 2; $S2_m$, RT measured for internal standard 2; and $S2_{fx}$, fixed standard RT of standard 2.

RESULTS

Optimization Experiments

The HPCE buffer originally introduced (2) was further optimized by replacing the organic modifier, 1,4-diaminobutane, with 1,5-diaminopentane, which resulted in an improved resolution of the hydrazinolysis-derived AGP *N*-glycan pool (Fig. 1). Increasing the tem-

perature (i.e., decreasing the viscosity of the buffer and increasing the electric current, respectively) increased the overall mobility of the *N*-glycan species, i.e., decreasing RT and the resolution of the peaks (not shown). The temperature proved optimal at 30°C.

Validation Experiments

The total hydrazinolysis-derived AGP *N*-glycan pool (2) (Fig. 1) was used as a panel of sialylated *N*-glycans for a series of validation experiments. This pool was repeatedly measured in 48 consecutive runs using four different buffer reservoirs and taking the buffer peak (S1) and the Neu5Ac peak (S2) as internal standards. Seventeen of the approximately 40 different peaks detected were evaluated with respect to their respective migration times. The separation and numbering of the peaks are presented in Fig. 1, and the overall mobility of the peaks, expressed as RT (min), is summarized in Table 1. As can be seen, the CV of the noncorrected peaks varied between 0.67 and 0.95%. The accuracy of the measurements could, however, be significantly improved by correcting the RT of the peaks via the two internal standards (Neu5Ac) and the buffer peak (which was, in this experiment, taken as the first internal standard). Thus, each of the 17 peaks was measured with a CV of <0.20%. Area and peak height of standard 2 (Neu5Ac) were evaluated and found to be accurate with a CV of less than 10% (not shown).

Accuracy of the Measurements

The necessity and efficiency of the use of two internal standards, such as MO (as a marker of the electroosmotic flow) and Neu5Ac, were further verified in numerous runs and are illustrated, by way of selected examples, in Table 2. These repetitive runs were performed weeks after the previous measurements, and dramatic shifts in RTs were observed from time to time, exhibiting CVs as high as 5%. While the correction of these RTs via MO alone (Correction 1) or Neu5Ac alone (Correction 2) provided significant improvements of the CV values, these were still in ranges much too high for reliable and repeatable measurements. However, the average of both corrected values (Correction 3) provided interassay variations with CV < 0.20% each time (Table 2), which were regarded as accurate and reliable enough for building the desired HPCE-mapping database.

The efficiency of the RT correction against two internal standards was further shown in a distinct series of experiments in which the effective length of the capillary was reduced to only half, which is illustrated by way of example in Table 3. As can be seen, the individual migration times of C4-446301.40 (as well as of the two internal standards) were also reduced to about half. However, their TCM values provided excellent agree-

TABLE 1

Validation Experiments Using the Hydrazinolysis-Derived AGP *N*-Glycan Pool as Standard Material in 48 Repetitive Runs

| Peak No. | 1 | Corr-01 | 2 | Corr-02 | 3 | Corr-03 | 4 | Corr-04 | 5 | Corr-05 | 6 | Corr-06 |
|---------------|-------|---------|-------|---------|-------|---------|-------|---------|-------|---------|-------|---------|
| RT-Aver (min) | 36.47 | 36.47 | 37.29 | 37.29 | 37.60 | 37.60 | 39.11 | 39.11 | 39.39 | 39.39 | 39.74 | 39.74 |
| StdDev (min) | 0.24 | 0.05 | 0.25 | 0.02 | 0.26 | 0.04 | 0.29 | 0.03 | 0.30 | 0.02 | 0.30 | 0.02 |
| CV (%) | 0.67 | 0.13 | 0.68 | 0.12 | 0.70 | 0.10 | 0.74 | 0.07 | 0.75 | 0.06 | 0.76 | 0.05 |
| Peak No. | 7 | Corr-07 | 8 | Corr-08 | 9 | Corr-09 | 10 | Corr-10 | 11 | Corr-11 | 12 | Corr-12 |
| Rt-Aver (min) | 40.00 | 40.00 | 40.91 | 40.91 | 41.33 | 41.33 | 41.61 | 41.61 | 42.28 | 42.28 | 42.63 | 42.63 |
| StdDev (min) | 0.30 | 0.02 | 0.32 | 0.02 | 0.33 | 0.02 | 0.34 | 0.02 | 0.35 | 0.02 | 0.36 | 0.03 |
| CV (%) | 0.76 | 0.04 | 0.79 | 0.04 | 0.80 | 0.04 | 0.81 | 0.04 | 0.83 | 0.05 | 0.84 | 0.07 |
| Peak No. | 13 | Corr-13 | 14 | Corr-14 | 15 | Corr-15 | 16 | Corr-16 | 17 | Corr-17 | S1 | S2 |
| RT-Aver (min) | 43.02 | 43.02 | 43.35 | 43.35 | 43.70 | 43.70 | 46.37 | 46.37 | 46.77 | 46.77 | 29.52 | 52.08 |
| StdDev (min) | 0.37 | 0.03 | 0.37 | 0.04 | 0.38 | 0.04 | 0.44 | 0.07 | 0.45 | 0.08 | 0.15 | 0.58 |
| CV (%) | 0.85 | 0.08 | 0.86 | 0.09 | 0.88 | 0.10 | 0.94 | 0.16 | 0.95 | 0.17 | 0.50 | 1.11 |

Note. RT-Av, average of the migration time; StdDev, standard deviation; CV, coefficient of variation; Corr-01–Corr-17, RT of peaks Nos. 1–17, corrected via the triple-correction method; S1, internal standard 1 (buffer peak); S2, internal standard 2 (Neu5Ac).

ment with the migration times contained in the HPCE-mapping database.

HPCE-Mapping Database

The migration times of the sialylated *N*-glycans, expressed as RTs (in min), are summarized in Table 4. Structures grouped according to their respective antennarity were clearly separated according to charge, i.e., their number of sialic acid residues. Tetraantennary (C4-*) structures exhibited RTs in the range of 35–44 min, i.e., 40–44 min (for C4-4* structures), 37–40 min (for C4-3* structures), and 35–37 min (for C4-2* structures). Triantennary (C3-*) structures appeared between 36.5 and 42 min, i.e., 39 and 42 min (C3-3* structures) and 36.5 and 37.5 min (C3-2* structures). Diantennary (C2-*) structures appeared between 33.5 and 39.5 min, i.e., 38 and 39.5 min (C2-2* structures) and 33.5 and 34.5 min (C2-1* structures).

Rules for Structural Alterations of *N*-Glycans

Some structural rules may be deduced from Table 4, expressed as RT shift differences (in min) observed upon structural alterations:

The removal of a single sialic acid residue was found to decrease the migration time of the respective *N*-glycan by ~3 min for tetraantennary (C4-4*), ~4 min for triantennary (C3-3*), and ~5 min for diantennary (C2-2*) structures, respectively.

The introduction of one or two LacNAc repeat(s) into C4-4* structures was found to decrease the migration time in the order of 1.2 and 2.2 min, respectively. The introduction of a LacNAc repeat into a C4-3* isomer shortened the RT by 1.0 min.

By analogy, the introduction of a Gal α 1,3 unit to OH-3 of the β -Gal residue of a C4-3* isomer shortened the migration time on the order of 0.4 min. The introduction of two Gal α 1,3 residues to the β -Gal termini of a C4-2* isomer decreased the RT by 0.8 min.

On the other hand, the removal of Gal β 1,4 from C2-124301.01.60. (Scheme 3), resulting in C2-114301.01.60., increased the migration time by 0.5 min.

The removal of Fuc α 1,6, attached to the proximal GlcNAc, resulted in an increase of the migration time by an average of 0.6 min.

The exchange of a single Neu5Ac by Neu5Gc in C2-224300.02 or C4-446301.40 did not influence the migration time.

The introduction into C2-224301.02 of a sulfate group to OH-6 of the GlcNAc of A2M3 (termed C2-224301.02.SO4-6N-A2M3) increased the migration time by 6.7 min.

Structural sialyl isomers carrying Neu5Ac α 2,3 linked to Gal migrated ~0.3 min faster than the corresponding α 2,6-isomers.

The Neu5Ac α 2,3-linked trisialo-triantennary fucosylated isomers (C3-335301.30.A4M3 and C3-335301.30.A6M6) were separated by 0.3 min (. . . A4M3 < . . . A6M6).

Structural Assignment of the *N*-Glycans of rhuEPO (BHK)

The PNGase F-derived *N*-glycan pool of rhuEPO (BHK) was separated into seven peaks (a–g) (Fig. 2). After correction of the peaks via the two internal stan-

TABLE 2

Migration Times in Repetitive Runs on Different Days of Selected *N*-Glycans and Their Corrections via the Two Internal Standards, Using the Triple-Correction Method

| Sample | Retention time (min) | | | | Sample | Sample TCM |
|---------------------------------------|----------------------|-------|-------|-------|--------|------------|
| | S1 | C-S1 | S2 | C-S2 | | |
| C4-446301.40 (3 runs) | | | | | | |
| RT-Aver | 29.83 | 42.70 | 52.67 | 42.86 | 42.62 | 42.78 |
| StdDev | 0.52 | 0.31 | 1.66 | 0.30 | 1.05 | 0.04 |
| CV (%) | 1.73 | 0.74 | 3.15 | 0.70 | 2.47 | 0.09 |
| C4-457301.40.1R-A2M6 (4 runs) | | | | | | |
| RT-Aver | 30.88 | 43.04 | 58.81 | 40.12 | 44.49 | 41.58 |
| StdDev | 0.76 | 1.03 | 4.05 | 0.93 | 2.12 | 0.05 |
| CV (%) | 2.45 | 2.39 | 6.89 | 2.32 | 4.76 | 0.12 |
| C4-468301.40.1R-A2M6.1R-A6M6 (2 runs) | | | | | | |
| RT-Aver | 30.14 | 40.58 | 53.55 | 40.49 | 40.93 | 40.54 |
| StdDev | 0.66 | 0.26 | 2.05 | 0.41 | 1.16 | 0.07 |
| CV (%) | 2.18 | 0.64 | 3.83 | 1.00 | 2.83 | 0.18 |
| C4-446301.31 (2 runs) | | | | | | |
| RT-Aver | 29.58 | 42.86 | 51.88 | 43.29 | 42.41 | 43.08 |
| StdDev | 0.01 | 0.02 | 0.06 | 0.04 | 0.01 | 0.01 |
| CV (%) | 0.03 | 0.05 | 0.11 | 0.09 | 0.02 | 0.02 |
| C4-457301.31.1R-A2M6 (4 runs) | | | | | | |
| RT-Aver | 30.70 | 42.85 | 57.26 | 40.79 | 44.03 | 41.82 |
| StdDev | 0.73 | 1.07 | 3.99 | 0.96 | 2.07 | 0.06 |
| CV (%) | 2.38 | 2.49 | 6.96 | 2.34 | 4.71 | 0.15 |
| C4-468301.31.1R-A2M6.1R-A6M6 (2 runs) | | | | | | |
| RT-Aver | 29.98 | 40.63 | 52.96 | 40.76 | 40.75 | 40.70 |
| StdDev | 0.54 | 0.28 | 1.76 | 0.34 | 1.02 | 0.03 |
| CV (%) | 1.81 | 0.69 | 3.32 | 0.83 | 2.50 | 0.07 |
| C3-335301.30.A4M3 (2 runs) | | | | | | |
| RT-Aver | 30.60 | 41.81 | 57.17 | 39.76 | 42.83 | 40.78 |
| StdDev | 0.90 | 0.96 | 4.53 | 1.07 | 2.24 | 0.06 |
| CV (%) | 2.94 | 2.30 | 7.93 | 2.70 | 5.24 | 0.14 |
| C2-224301.02 (4 runs) | | | | | | |
| RT-Aver | 31.83 | 40.46 | 62.02 | 36.80 | 43.08 | 38.63 |
| StdDev | 0.51 | 0.18 | 1.76 | 0.29 | 0.88 | 0.06 |
| CV (%) | 1.61 | 0.44 | 2.84 | 0.79 | 2.05 | 0.15 |
| C2-224300.02 (3 runs) | | | | | | |
| RT-Aver | 32.23 | 41.45 | 63.67 | 37.17 | 44.69 | 39.31 |
| StdDev | 0.12 | 0.10 | 0.30 | 0.09 | 0.16 | 0.01 |
| CV (%) | 0.39 | 0.24 | 0.47 | 0.24 | 0.37 | 0.02 |

Note. S1, internal standard 1 (mesityl oxide, MO); S2, internal standard 2 (Neu5Ac); C-S1, RT of the sample, corrected via standard 1; C-S2, RT of the sample, corrected via standard 2; TCM, RT of the sample, corrected via the triple-correction method; Aver, average of the migration time; StdDev, standard deviation; CV, coefficient of variation.

dards (using the triple-correction method), each peak could be assigned as distinct *N*-glycan structure by comparison with the HPCE-mapping database, which is summarized in Table 5. For peak f, two different structures were revealed by the mapping database, accounting for the possible superposition of C4-457301.40.1R-A2M6 and C3-335301.30.A6M6, which was confirmed via the detailed carbohydrate structural analysis (7). The superposition of these two peaks may account for their relatively high RT deviation (i.e., between 0.20 and 0.27%) from the RT values contained in the HPCE-mapping database.

Structural Assignment of the *N*-Glycans of Bovine Serum Fetuin

The hydrazinolysis (GlycoPrep 1000)-derived glycan pool of the fetuin sample was separated into about 15 different peaks, 14 of which are indicated by the letters a–n (Fig. 3). Nine of these 14 peaks could be assigned as sialylated *N*-glycans by comparing their respective TCM values with the TCM values contained in the HPCE-mapping databases (Table 6). The occurrence of these structures on fetuin was confirmed by comparison with the fetuin *N*-glycan structures described in the lit-

TABLE 3

Migration Times in Repetitive Runs on Different Days of C4-446301.40, Using Two Capillaries of Different Length, and Their Corrections via the Two Internal Standards, Using the Triple-Correction Method

| Run | Sample | Migration time (min) | | | |
|-----|--------------|----------------------|-------------|-----------------|------------------|
| | | S1 (MO) | S2 (Neu5Ac) | Sample measured | Sample corrected |
| 1 | C4-446301.40 | 29.55 | 52.02 | 42.10 | 42.72 |
| 2 | C4-446301.40 | 30.55 | 54.95 | 44.08 | 42.81 |
| 3 | C4-446301.40 | 29.38 | 51.05 | 41.67 | 42.81 |
| 4 | C4-446301.40 | 14.07 | 26.12 | 20.60 | 42.77 |
| 5 | C4-446301.40 | 14.05 | 26.05 | 20.58 | 42.81 |

Note. Abbreviations as in Table 2.

erature (13–15). (Reminder: The fetuin O-glycan structures were largely removed during the desalting step.)

Structural Assignment of the N-Glycans of α_1 -Acid Glycoprotein

After the establishment of the mapping database, 20 of about 40 peaks of the manual (large-scale; 50 mg) hydrazinolysis-derived AGP N-glycan pool (2) of Fig. 1 could retrospectively be assigned by comparison with the mapping database, which is summarized in Table 7. As can be seen, the C4-446300.?? sialyl isomers (peaks 12–15) are clearly separated according to the number of α 2,3- and α 2,6-linkages. The groups of the C4-4* (peaks 12–15), C3-3* (peaks 8–10), and C2-2* (peak 4) structures are separated by about 2 and 3 min, respectively. The groups of the C4-4* (peaks 12–15), C4-3* (peaks 6 and 7) and C4-2* (peak 1) structures are similarly separated by about 3 min each. The migration time of N-gly-

cans of a given charge is decreased with increasing size, showing the following order of migration: C4-2* (peak 1) < C3-2* (peak 3) < C2-2* (peak 4), and C4-3* (peaks 6 and 7) < C3-3* (peaks 8–10), respectively.

The groups of peaks seen in the peak 16–17 region (Fig. 1) were found to relate to glycopeptide fragments formed during hydrazinolysis. This was apparent from a more detailed analysis of the MQ-5 fraction earlier isolated via Mono-Q FPLC (2). To this, the desalted MQ-5 fraction of a large-scale hydrazinolysis (1000 mg of AGP (2)) was recovered (yielding 11 mg; ~1% of the total AGP by weight) and subjected to PNGase F treatment. The released N-glycans of the MQ-5 fraction were analyzed via high-resolution ^1H NMR, HPAE-PAD, and HPCE and identified as the regular (nonsulfated) N-glycans also seen in the AGP large-scale N-glycan pool (unpublished results).

Comparison of Two Different HPCE Systems

The large-scale (50 mg) hydrazinolysis-derived AGP N-glycan pool was measured five times on 4 different days using the ABI 270A-HT apparatus. As can be seen from Table 7, the measured (noncorrected) average migration times of peaks 1–14 varied with an interassay variation that continuously increased from 2.38% (for peak 1) to 2.80% (for peak 14). However, the averages of the TCM-corrected migration times were accurate with an interassay variation of less than 0.30% and have therefore entered the mapping database. Interestingly, the accuracy of the corrected average migration times improved from peak 1 (CV 0.27%) to peak 10 (CV 0.08%) and then slightly decreased again, proceeding to peak 14 (CV 0.22%), which corresponds with the results of the validation experiment summarized in Table 1.

The same sample of AGP N-glycan pool was remeasured about 3 years later (different laboratory, different

TABLE 4

Average Migration Time Shifts Observed upon Structural Alterations of Sialylated N-Glycans, as Deduced from the HPCE-Mapping Database

| | RT (min) | -Neu5Ac | +1R | +2R | +1G | +2G | +F prox | +SO ₄ | -Ac+Gc | -Gal |
|-------|-----------|---------|------|------|------|------|---------|------------------|--------|------|
| C4-* | | | | | | | | | | |
| C4-4* | 40–44 | -3 | -1.2 | -2.2 | | | -0.6 | | ±0 | |
| C4-3* | 37–40 | | -1.0 | | -0.4 | | | | | |
| C4-2* | 35–37 | | | | | -0.8 | | | | |
| C3-* | | | | | | | | | | |
| C3-3* | 39–42 | -4 | | | | | -0.6 | | | |
| C3-2* | 36.5–37.5 | | | | | | -0.5 | | | |
| C2-* | | | | | | | | | | |
| C2-2* | 38–39.5 | -5 | | | | | -0.7 | +6.7 | ±0 | |
| C2-1* | 33.5–34.5 | | | | | | -0.5 | | | +0.5 |

Note. +1R(2R), +1(+2) N-acetylglucosamine repeat(s); +1G(2G), +1(+2) galactose- α 1,3-residue(s); +F, +1 fucose (α 1,6-linked to the proximal GlcNAc); +SO₄, + sulfate; -Ac/+Gc, N-acetyl replaced by N-glycolyl; -Gal, removal of a β 1,4-linked galactose residue.

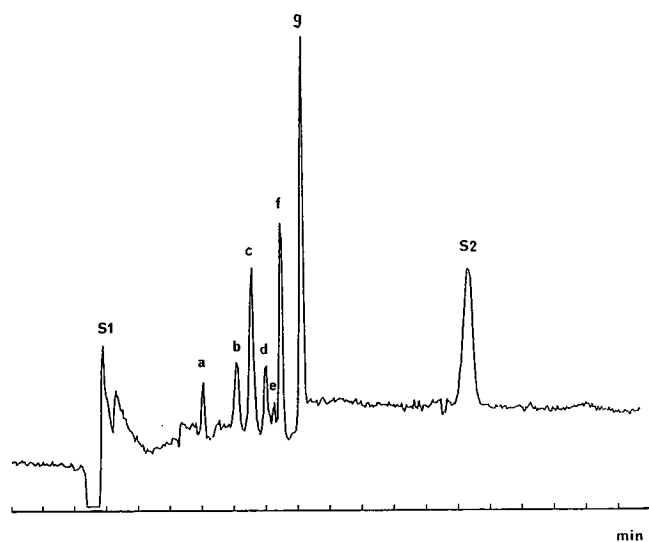


FIG. 2. Electropherogram of the PNGase F-derived *N*-glycan pool of rhuEPO (BHK). S1, internal standard 1 (mesityl oxide); S2, internal standard 2 (Neu5Ac).

analyst) using the Beckman 5500 P/ACE system. These results are also shown in Table 7. As can be seen, the TCM-corrected migration times of this measurement were in excellent agreement with the peak average values of the 270A-HT measurements contained in the mapping database. The deviation from the (average) 270A-HT database values of the P/ACE peaks proved to be less than 0.25% each, except peak 1, for which the deviation from the database value was 0.41%. An extraordinary agreement with the TCM-corrected database values was observed for peaks 8–10, providing deviations of less than 0.10% each.

DISCUSSION

We have recently introduced a mapping database for *N*-glycans that enables structural assignment by mere

comparison of retention times using high-pH anion-exchange chromatography with pulsed amperometric detection (1). The comparison of the structures with *N*-glycans contained in the mapping database was greatly facilitated by using the nomenclature and abbreviations introduced to enable proper search profiles in the mapping database (1), which is outlined in Schemes 1–3.

In the search for an appropriate alternative mapping dimension, we have developed new buffers and conditions that allow separation and detection of sialylated *N*-glycans by HPCE with uv detection at 190 nm (2), requiring neither borate complex formation (16–23) nor carbohydrate derivatization (16–19,22,24–26) for successful separation and detection. (For a recent review see Ref. 27.) Thus, we have been able to separate the hydrazinolysis-derived *N*-glycan pool of human plasma AGP into approx 40 distinct peaks (2). The carbonyl functions of the *N*-acetyl and carboxyl groups present in these molecules enable direct uv detection at 190 nm at concentrations in the femtomole region, consuming about 4000 times less material than the corresponding measurements by HPAE–PAD (2). This is best reflected by the sample volumes injected (at identical concentrations), i.e., 5 nl HPCE and 20 μ l HPAE–PAD, respectively. Despite the very low amounts of nonderivatized material consumed for the actual measurement (i.e., 5 nl each, equivalent to \sim 100 fmol/*N*-glycan), the sample processing and preparation, of course, require volumes on the order of microliters.

While this work was in progress, Taverna *et al.* (28) have independently shown that nonderivatized sialylated *N*-glycans could be separated in HPCE in 50 mM Tricine/2.5 mM putrescine, pH 8.2, at 20°C or in 200 mM borate/1.25 mM putrescine, pH 8.2, at 30°C and detection at 200 nm. In these experiments, and in contrast to our approach, the capillary surface had to be modified with 3-mercaptopropyltrimethoxysilane, prior to use. No data were provided on the accuracy of this method. However, when the glycopeptides “GP2” of rt-PA were

TABLE 5

Analysis of the PNGase F-Derived *N*-Glycan Pool of rhuEPO (BHK) by Comparison with Structures Contained in the HPCE-Mapping Database

| Peak No. | Identified structure | RT (min) measured | RT (min) corrected | Derivation from database value |
|----------|------------------------------|-------------------|--------------------|--------------------------------|
| a | C4-246301.20 | 17.16 | 36.11 | <0.10% |
| b | C4-357301.30.1R-A2M6 | 18.27 | 38.44 | <0.20% |
| c | C4-346301.30.0333. | 18.73 | 39.41 | <0.20% |
| d | C4-468301.40.1R-A2M6.1R-A6M6 | 19.15 | 40.30 | <0.16% |
| e | C3-335301.30.A4M3 | 19.40 | 40.82 | <0.10% |
| f | C4-457301.40.1R-A2M6 | 19.63 | 41.31 | <0.27% |
| | C3-335301.30-A6M6 | 19.63 | 41.31 | <0.25% |
| g | C4-446301.40 | 20.32 | 42.76 | <0.13% |

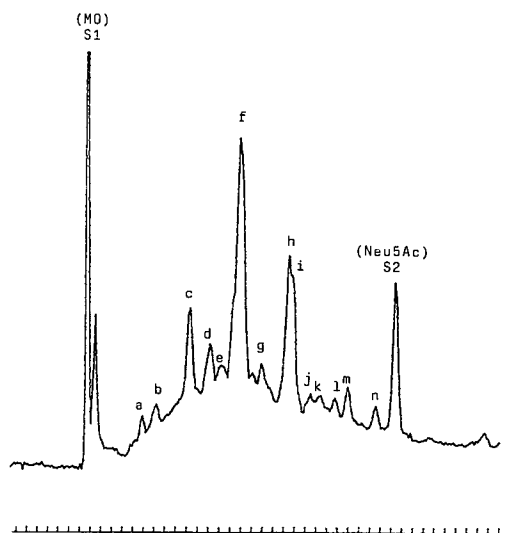


FIG. 3. Electropherogram of the automated hydrazinolysis-derived glycan pool of bovine serum fetuin. S1, internal standard 1 (mesityl oxide); S2, internal standard 2 (Neu5Ac).

measured in 150 mM borate buffer, pH 9.0–9.2, or 100 mM phosphate buffer, pH 6.6, the CV was less than 1.4 and 1.7–2.0%, respectively. In the presence of 2.5 mM putrescine, the CV was even higher, i.e., less than 2.3% (28).

Here we describe an optimized HPCE buffer system and conditions that allow separation and detection at 190 nm of nonderivatized sialylated *N*-glycans with a coefficient of variation of usually less than 0.20%, which

is about four times more accurate than the method recently communicated by Suzuki *et al.* (29) for the measurements of pyridyl-aminated asialo-*N*-glycans. These authors have used PA-glucose as internal standard for appropriate corrections of the measured migration times, which provided CV = 0.80%, with 100 mM phosphate buffer, pH 2.5, in the presence of 0.1% (w/w) hydroxypropylcellulose, and CV = 0.50%, with 200 mM borate buffer, pH 10.5.

In the course of our investigation, we have found that the use of a single internal standard did not ensure correct measurements, especially when the measurements were repeated on different days weeks apart. However, this serious drawback could be overcome using a second internal standard and (what may be termed) a “triple-correction method,” in which the measured RT of the carbohydrate is corrected (i) against the first internal standard (Eq. [1]) and (ii) against the second internal standard (Eq. [2]), after which (iii) the average of these two corrected values is calculated (Eq. [3]). Moreover, this triple-correction method has as a prerequisite the properly determined RTs of the two internal standards as reference values.

As can be seen from Table 2, the average RT of C4-446301.40 in three different runs was 42.62 ± 1.05 min (2.47%). The correction (i) against the first internal standard, MO, improved the RT to 42.70 ± 0.31 min (0.74%); the correction (ii) against the second internal standard, Neu5Ac, improved the RT to 42.86 ± 0.30 min (0.70%); and the average (iii) of the two corrected values further improved the RT to 42.78 ± 0.04 min (0.09%).

Similarly, the average RT of C4-457301.40.1R-A2M6

TABLE 6

Analysis of the Automated Hydrazinolysis-Derived Glycan Pool of Bovine Serum Fetuin by Comparison with Structures Contained in the HPCE-Mapping Database

| Peak No. | Identified structure | RT (min) measured | RT (min) corrected | Deviation from database value (%) |
|----------|--|----------------------|-----------------------|---|
| a | C3-124300.??A4M3 | 36.38 | 33.46 | <0.25 |
| b | C2-124300.01.?? | 37.70 | 34.67 | <0.50 |
| c | C3-235300.??A4M3 | 40.80 | 37.52 | <0.16 |
| d | C2-224300.02 | 42.79 | 39.35 | <0.10 |
| e | No hit | 43.78 | 40.26 | |
| f | C3-335300.12.A4M3.663. | 45.58 | 41.92 | <0.10 |
| g | No hit | 47.58 | 43.75 | |
| h | C3-435300.22.A4M3* ^a | 50.23 | 46.19 | <0.50 |
| i | C3-435300.13.A4M3* ^b | 50.53 | 46.47 | <0.25 |
| j | No hit | 52.18 | 47.98 | |
| k | No hit | 53.00 | 48.74 | |
| l | C3-535300.23.A4M3* ^c | 54.57 | 50.18 | <0.10 |
| m | O-Glycan tetrasaccharide (disialylated Gal β 1, 3GalNAc) | 55.75 | 51.26 | <0.10 |
| n | No hit | 58.38 | 53.69 | |

*^{a,b} Sialyl isomers with one Neu5Ac residue α 2,6-linked to GlcNAc on the A4M3 branch, which carries Gal β 1,3GlcNAc.

*^c Sialyl isomer with two Neu5Ac residues α 2,6-linked to GlcNAc on the A2M6 and the A4M3 branch, which both carry Gal β 1,3GlcNAc.

TABLE 7

N-Glycan Structures Tentatively Assigned for the Hydrazinolysis-Derived AGP *N*-Glycan Pool, Their Average TCM-Values (Five Runs at 4 Different Days (270A-HT System, ABI), and the Comparison Using a Different HPCE-System (Beckman, 5500 P/ACE; Different Analyst, Different Laboratory)

| Peak No. ^a | Assigned structure | Applied Biosystems 270A-HT | | | | | | Beckman 5500 P/ACE | | | |
|-----------------------|--------------------|----------------------------|--------------|--------|--------------------------|--------------|--------|--------------------|-----------|-----------|---------|
| | | Database value measured | | | Database value corrected | | | RT (min) | TCM (min) | Dev (min) | Dev (%) |
| | | Av (min) | StdDev (min) | CV (%) | Av (min) | StdDev (min) | CV (%) | | | | |
| 1 | C4-246300.?? | 41.25 | 0.98 | 2.38 | 36.19 | 0.10 | 0.27 | 37.77 | 36.04 | 0.15 | 0.41 |
| 3 | C3-235300.??A4M3 | 42.74 | 1.06 | 2.48 | 37.49 | 0.08 | 0.21 | 39.21 | 37.41 | 0.07 | 0.20 |
| 4 | C2-224300.02 | 44.83 | 1.13 | 2.53 | 39.32 | 0.05 | 0.12 | 41.14 | 39.26 | 0.06 | 0.16 |
| 6 | C4-346300.?? | 45.67 | 1.18 | 2.58 | 40.06 | 0.04 | 0.10 | 41.93 | 40.01 | 0.05 | 0.14 |
| 7 | C4-346300.?? | 46.02 | 1.19 | 2.58 | 40.37 | 0.04 | 0.10 | 42.25 | 40.31 | 0.06 | 0.15 |
| 8 | C3-335300.21.A4M3 | 47.30 | 1.27 | 2.68 | 41.49 | 0.04 | 0.10 | 43.49 | 41.50 | -0.01 | -0.03 |
| 9 | C3-335300.12.A4M3 | 47.89 | 1.30 | 2.71 | 42.01 | 0.04 | 0.09 | 44.03 | 42.01 | 0.00 | -0.01 |
| 10 | C3-335300.03.A4M3 | 48.27 | 1.29 | 2.68 | 42.34 | 0.03 | 0.08 | 44.40 | 42.37 | -0.03 | -0.06 |
| 12 | C4-457300.??1R | 49.71 | 1.38 | 2.77 | 43.60 | 0.08 | 0.17 | 45.77 | 43.67 | -0.07 | -0.16 |
| 13 | C4-446300.31 | 50.26 | 1.41 | 2.80 | 44.08 | 0.09 | 0.21 | 46.30 | 44.18 | -0.10 | -0.22 |
| 14 | C4-446300.22 | 50.73 | 1.42 | 2.80 | 44.50 | 0.10 | 0.22 | 46.71 | 44.57 | -0.07 | -0.16 |

^a Peak numbering as shown in Fig. 1.

in four different runs was 44.49 ± 2.12 min (4.76%). This large CV value is due to the great deviation of the first run from the three other runs. The correction (i) against the first internal standard, MO, improved the RT to 43.04 ± 1.03 min (2.39%); correction (ii) against the second internal standard, Neu5Ac, improved the RT to

40.12 ± 0.93 min (2.32%); and the average (iii) of the two corrected values finally improved the RT to 41.58 ± 0.05 min (0.12%). These two examples (further examples may be deduced from Table 2) clearly prove the efficiency of the triple-correction method, which is the subject of a patent application filed by Behringwerke AG.

The optimized HPCE standard conditions and the triple-correction method were used to extensively validate the HPCE-mapping procedure (Table 1) and to establish a validated HPCE-mapping database.

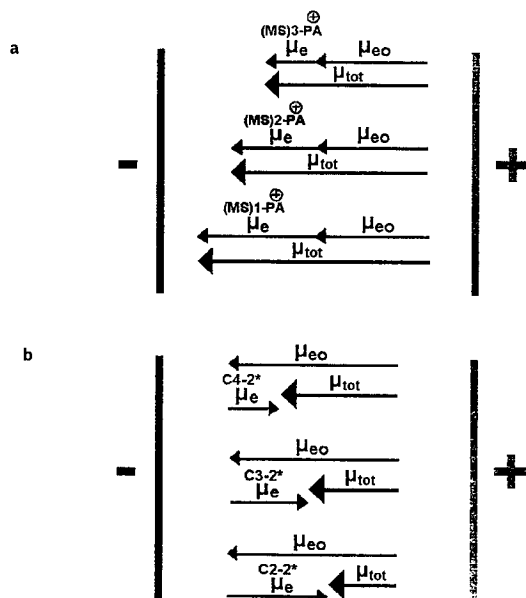
Theoretical Considerations

When positively charged carbohydrate derivatives are applied at the anodic side (e.g., amino derivatives at acidic pH), such as 2-AP- (18,19,25,26) or 6-AQ-derivatives (25), both the electrophoretic and the electroosmotic mobility are directed toward the cathode and add to the overall mobility of the solutes. When negatively charged carbohydrates are applied at the anodic side, such as sulfated (21,23,27,30) or sialylated structures (2,28) or AGA derivatives of neutral structures (22) or sugar alcoholates obtained at pH 9.4 (31), the electrophoretic mobility is toward the anode. The solutes are prevented from migrating back off the capillary by the electroosmotic flow that carries them toward the cathode.

The electrophoretic mobility μ of a molecule is characterized by

$$\mu = v/E = q/6\pi\nu r, \quad [4]$$

where v is the migration velocity, E is the electric field strength, q is the net charge on the molecule, ν is the



SCHEME 4. Mobility of charged carbohydrates. (a) Mobility of positively charged (pyridyl-aminated) saccharides of a homologous series. (b) Mobility of negatively charged (sialylated) di-, tri-, and tetraantennary *N*-glycans.

solvent viscosity, and r is the apparent Stokes radius of the molecule (32). Thus, the electrophoretic mobility will decrease with increasing size of the molecules. Hence, when the carbohydrate is carrying a positive charge, the electrophoretic mobility (μ_e) toward the cathode (i.e., the same direction as the electroosmotic flow, μ_{eo}) will decrease with increasing Stokes radius, as the larger molecules are more retarded by their friction in the buffer. Therefore, the overall mobility (μ_{tot}) of positively charged carbohydrates of a homologous series will decrease with an increasing degree of polymerization (Scheme 4a) (see Refs. 18,19,25). In contrast, when the carbohydrate is carrying a negative charge, the electrophoretic mobility (μ_e) toward the anode (i.e., the opposite direction as the electroosmotic flow, μ_{eo}) will decrease with increasing Stokes radius, as the larger molecules are more efficiently carried toward the cathode via the electroosmotic flow, due to their increased friction in the buffer. Therefore, the overall mobility (μ_{tot}) of negatively charged carbohydrates will increase with increasing degree of polymerization (see Refs. 22,31) or size (i.e., the Stokes radius; Scheme 4b), which helps to rationalize the RT-shift differences observed between distinct *N*-glycan structures of the HPCE-mapping database (Table 4).

Structural Alterations

Based on the approximately 80 sialylated *N*-glycan structures that have thus far entered the database, valuable rules that make it possible to predict RT shifts that must be expected upon structural alterations can be drawn:

The introduction of one or two LacNAc repeats (e.g., into C4-4* structures), one or two Gal α 1,3 residues (e.g., into C4-3* and C4-2* structures, respectively), or fucose (e.g., α 1,6 linked to the proximal GlcNAc) resulted in increased overall mobilities, i.e., reduced migration times (Table 4). In other words, the enlarged *N*-glycans of a given charge were more quickly carried away with the electroosmotic flow.

From the RT shifts summarized in Table 4, one is tempted to conclude that under the standard conditions described, the introduction of a monosaccharide unit, such as Gal or Fuc, will decrease the RT of a given *N*-glycan of a given charge by 0.5–0.6 min. Similarly, the introduction of two or four monosaccharide units, i.e., the introduction of one or two LacNAc repeats, will decrease the RT by $2 \times (0.5-0.6) \text{ min} = 1.0-1.2 \text{ min}$ and $4 \times (0.5-0.6) \text{ min} = 2.0-2.4 \text{ min}$, which is actually observed.

Our finding (Table 4) that the replacement of Neu5Ac by Neu5Gc does not affect the RT is quite reasonable, as the apparent Stokes radius remains unchanged. This is quite different from the separation of these molecules

by HPAE-PAD, where the replacement of *N*-acetyl by *N*-glycolyl results in a dramatic increase of the RT (1), due to the introduction of an OH group that is considerably acidified by the neighboring carbonyl function.

More difficult to explain is why sialyl isomers in which an α 2,6-linked Neu5Ac is replaced by an α 2,3-linked Neu5Ac migrate about 0.3 min faster, which is in contrast to what is observed by HPAE-PAD (1). The suggestion that in α 2,3-linked sialyl isomers the apparent Stokes radius is somewhat larger than that in the corresponding α 2,6-linked analogue needs further confirmation.

The removal of negative charge reduces the electrophoretic mobility of the *N*-glycans toward the anode (Eq. [4]) and thus reduces the migration time toward the cathode (Scheme 4b). This effect was more pronounced with diantennary structures (–5 min) than with triantennary (–4 min) and tetraantennary structures (–3 min). Obviously, the loss of specific charge (expressed by the charge-to-mass ratio) decreases in the order di- (one charge per two antennae) > tri- (one charge per three antennae) > tetraantennary structures (one charge per four antennae), concomitant with a decrease of the electrophoretic mobility toward the anode in the order di- > tri- > tetraantennary structures, corresponding with an increase of the overall mobility toward the cathode in the same order.

Surprisingly, the triantennary C3-335301.30.A4M3 eluted about 0.3 min earlier than the corresponding C3-335301.30.A2M6 isomer, whereas these isomers were not separated by HPAE-PAD (1). Further experiments and calculations will have to show whether the apparent Stokes radius of the A4M3 isomer is slightly increased.

Whereas the introduction of Neu5Ac into C3-2* increased the RT by ~ 4 min, the introduction of a sulfate group into C2-224301.20 increased the RT by ~ 6.7 min, which reflects the greater acidity of sulfuric versus sialic acid.

In general, both the removal of charge and the increase in size reduce the migration time of the negatively charged *N*-glycans. Our (originally surprising) finding that the migration time of free Neu5Ac was even larger than the RTs of the tetrasialylated structures (2) (Fig. 1) is now easily explained, as the specific charge (charge to apparent Stokes radius ratio) of Neu5Ac is larger than that of any of the tetrasialylated *N*-glycans.

Noteworthy, we have found that peaks 16 and 17 of the hydrazinolysis-derived AGP *N*-glycan pool (Fig. 1), which were originally presumed to be sulfated *N*-glycans (2), were, in fact, glycopeptide fragments that have not been cleaved during the manual (large-scale) hydrazinolysis. This was ascertained via PNGase F digestion of the Mono-Q fraction “MQ-5” previously isolated (2) and subsequent analysis of the liberated *N*-glycans via high-resolution ^1H NMR spectroscopy, HPCE, and

HPAE-PAD (unpublished results). This observation demonstrates some limitation of HPCE in using non-derivatized carbohydrates, gained via hydrazinolysis, as (glyco)peptide fragments may erroneously be regarded as nonderivatized *N*-glycans. Throughout the present investigation, however, the nonderivatized *N*-glycans were clearly spiked on top of the peptide-derived baseline "hill" (Figs. 1 and 3), attributable to the hydrazinolysis-derived peptide fragments, whereas a straight baseline is observed for *N*-glycans liberated via PNGase F digest (Fig. 2). Therefore, it is suggested that HPCE-mapping databases of appropriately derivatized glycans, established using the triple-correction method outlined herein, may prove more reliable (with respect to the carbohydrate-specific peak assignment) than this current mapping database of nonderivatized *N*-glycans.

Structural Assignment of N-Glycans via the HPCE-Mapping Database

To verify the suitability and reliability of the database for the structural determination of sialylated *N*-glycans by mere comparison of migration times, *N*-glycan pools of various glycoproteins were measured by HPCE under the optimized conditions. The comparison of the triple-corrected migration times with the triple-corrected migration times of known *N*-glycans contained in the HPCE-mapping database was straightforward. Thus, all seven peaks of the PNGase F-derived *N*-glycan pool of rhuEPO (BHK) (Fig. 2 and Table 5) and 9 of the approximately 15 peaks of bovine serum fetuin could be assigned as distinct glycan structures (Fig. 3, Table 6) by comparison with the HPCE-mapping database. Noteworthy, the reducing disialylated and monosialylated *O*-glycan structures (disialylated and monosialylated Gal β 1,3GalNAc) are separated under these HPCE conditions by approx 10 min, whereas they are degraded to the "peeled" disaccharide NeuAca2,3-Gal under the HPAE-PAD mapping conditions previously described (1) (unpublished results).

About two-thirds of the peaks in the chromatogram of the hydrazinolysis-derived AGP *N*-glycan pool (Fig. 1) could tentatively be assigned as distinct *N*-glycans by comparison with the HPCE-mapping database (Table 7), taking into account, however, that the groups of peaks seen in the peak 16–17 region are attributable to glycopeptide fragments (unpublished results).

Finally, it could be shown that the database values hold true not only for the HPCE apparatus with which the database was created (Applied Biosystems 270A-HT), but also for measurements performed by a different analyst in a different laboratory using a different HPCE system (the Beckman 5500 P/ACE; Table 7). Therefore, we are convinced that the TCM-corrected values of the HPCE-mapping database may also hold

true for measurements performed with still other HPCE systems and in still other laboratories, provided the measurements are performed under validated conditions.

CONCLUSIONS

The separation of *N*-glycans according to charge and size by mere migration in an electric field, not requiring interaction with either an ion-exchange resin or another separation matrix, exhibits clear advantages with respect to the accuracy and reproducibility of the migration times.

From the high accuracy of the measurements achieved with the triple-correction method, we are convinced that the corrected migration times of nonderivatized glycans, as well as those of appropriately derivatized carbohydrates, are generally suitable for the establishment of HPCE-mapping databases, which opens a new method for the carbohydrate structural assignment by mere comparison of migration times.

In our hands, the analysis of nonderivatized *N*-glycans via HPAE-PAD (1) (as the first dimension) and HPCE (as the second dimension) and the comparison with the established mapping databases have proven to constitute the simplest and quickest technique for the structural assignment of sialylated *N*-glycans available to date.

ACKNOWLEDGMENT

We are obliged to Ralf Bauer for performing the measurements on the Beckman 5500 P/ACE system.

REFERENCES

1. Hermentin, P., Witzel, R., Vliegthart, J. F. G., Kamerling, J. P., Nimitz, M., and Conradt, H. S. (1992) *Anal. Biochem.* **203**, 281–289.
2. Hermentin, P., Witzel, R., Doenges, R., Bauer, R., Haupt, H., Patel, T., Parekh, R. B., and Brazel, D. (1992) *Anal. Biochem.* **206**, 419–429.
3. Conradt, H. S., Egge, H., Peter-Katalinic, J., Reiser, W., Siklosi, T., and Schaper, K. (1987) *J. Biol. Chem.* **262**, 14600–14605.
4. Zettlmeißl, G., Conradt, H. S., Nimitz, M., and Karges, H. E. (1989) *J. Biol. Chem.* **264**, 21153–21159.
5. Nimitz, M., Noll, G., Paques, E.-P., and Conradt, H. S. (1990) *FEBS Lett.* **271**, 14–21.
6. Nimitz, M., and Conradt, H. S. (1991) in *Protein Glycosylation: Cellular, Biotechnological and Analytical Aspects*, GBF Monographs (Conradt, H. S., Ed.), Vol. 15, pp. 235–248, VCH Publishers, Weinheim/New York/Cambridge.
7. Nimitz, M., Martin, W., Wray, V., Klöppel, K.-D., Augustin, J., and Conradt, H. S. (1993) *Eur. J. Biochem.* **213**, 39–56.
8. Vliegthart, J. F. G., Dorland, L., and Van Halbeek, H. (1983) *Adv. Carbohydr. Chem. Biochem.* **41**, 209–374.
9. Hokke, C. H., Bergwerff, A. A., van Dedem, G. W. K., van Oostrum, J., Kamerling, J. P., and Vliegthart, J. F. G. (1990) *FEBS Lett.* **275**, 9–14.

10. Vliegthart, J. F. G., Hård, K., de Waard, P., and Kamerling, J. P. (1991) in *Protein Glycosylation: Cellular, Biotechnological and Analytical Aspects*, GBF Monographs (Conradt, H. S., Ed.), Vol. 15, pp. 137-146, VCH Publishers, Weinheim/New York/Cambridge.
11. Hokke, C. H., Kamerling, J. P., van Dedem, G. W. K., and Vliegthart, J. F. G. (1991) *FEBS Lett.* **286**, 18-24.
12. De Waard, P., Koorevaar, A., Kamerling, J. P., and Vliegthart, J. F. G. (1991) *J. Biol. Chem.* **266**, 4237-4243.
13. Green, E. D., Adelt, G., Baenzinger, J. U., Wilson, S., and Van Halbeek, H. (1988) *J. Biol. Chem.* **263**, 18253-18268.
14. Bendiak, B., Harris-Brandts, M., Michnick, S. W., Carver, J. P., and Cumming, D. A. (1989) *Biochemistry* **28**, 6491-6499.
15. Cumming, D. A., Hellerqvist, C. G., Harris-Brandts, M., Michnick, S. W., Carver, J. P., and Bendiak, B. (1989) *Biochemistry* **28**, 6500-6512.
16. Nashabeh, W., and El Rassi, Z. (1991) *J. Chromatogr.* **536**, 31-42.
17. Honda, S., Iwase, S., Makino, A., and Fujiwara, S. (1989) *Anal. Biochem.* **176**, 72-76.
18. Honda, S., Makino, A., Suzuki, S., and Kakehi, K. (1990) *Anal. Biochem.* **191**, 228-234.
19. Nashabeh, W., and El Rassi, Z. (1990) *J. Chromatogr.* **514**, 57-64.
20. Hoffstetter-Kuhn, S., Paulus, A., Gassmann, E., and Widmer, H. M. (1991) *Anal. Chem.* **63**, 1541-1547.
21. Al-Hakim, A., and Linhardt, R. J. (1991) *Anal. Biochem.* **195**, 68-73.
22. Lee, K.-B., Kim, Y.-S., and Linhardt, R. J. (1991) *Electrophoresis* **12**, 636-640.
23. Carney, S. L., and Osborne, D. J. (1991) *Anal. Biochem.* **195**, 132-140.
24. Honda, S., Yamamoto, K., Suzuki, S., Ueda, M., and Kakehi, K. (1991) *J. Chromatogr.* **588**, 327-333.
25. Nashabeh, W., and El Rassi, Z. (1992) *J. Chromatogr.* **600**, 279-287.
26. Honda, S., Suzuki, S., Nose, A., Yamamoto, K., and Kakehi, K. (1991) *Carbohydr. Res.* **215**, 193-198.
27. Linhardt, R. J. (1994) *Methods Enzymol.* **230**, 265-280.
28. Taverna, M., Baillet, A., Biou, D., Schlüter, M., Werner, R., and Ferrier, D. (1992) *Electrophoresis* **13**, 359-366.
29. Suzuki, S., Kakehi, K., and Honda, S. (1992) *Anal. Biochem.* **205**, 227-236.
30. Ampofo, S. A., Wang, H. M., and Linhardt, R. J. (1991) *Anal. Biochem.* **199**, 249-255.
31. Liu, J., Shirota, O., and Novotny, M. (1991) *Anal. Chem.* **63**, 413-417.
32. Tran, A. D., Park, S., Lisi, P. J., Huynh, O. T., Ryall, R. R., and Lane, P. A. (1991) *J. Chromatogr.* **542**, 459-471.